WILEY-VCH

Supporting Information

Large-scale synthesis of size- and thickness-tunable conducting polymer nanosheets *via* a salt-templated method

Liang Huang, ‡ Zhengfeng Guo, ‡ Kaisi Liu, Xiong Liukang, Liwei Huang, Xiang Gao, Jiabin Wu, Jun Wan, Zhimi Hu, and Jun Zhou*

Wuhan National Laboratory for Optoelectronics, Huazhong University of Science and Technology, Wuhan 430074, P. R. China. Correspondence and requests for materials should be addressed to J. Z. (email: jun.zhou@mail.hust.edu.cn).

Materials and method:

All the materials for synthesis were purchased from commercial suppliers and used without further purification.

The integrated-average gravimetric capacitance of each electrode was calculated from the CV data according to:

$$C_g = \frac{2}{s \times m \times V}\left(\int_{1.6}^{0} jdV\right)[F/g]$$

$$C_v = C_g \times \rho[F/cm^3]$$

where C_g-normalized specific capacitance (F/g), C_v-volumetric capacitance (F/cm^3), ρ-mass density (g/cm^3), j-total current (A), s-scan rate (V/s), V-voltage window (V), m-mass of each electrode.

The energy E (Wh /L^{-1}) and power P (W /L^{-1}) densities of the symmetric device were estimated as:

$$E = \frac{C_v \times V^2}{8 \times 3.6}[Wh/L]$$

$$P = \frac{E \times 3600 \times s}{V}[W/L]$$

The specific capacitance was calculated from the galvanostatic charge and discharge curves, using the following equations :

$$SC = \frac{J\,t}{m\Delta V}$$

where J is charge or discharge current, t is the time for a full discharge, m indicates the mass of the active material, and ΔV represents the voltage change after a full charge or discharge.

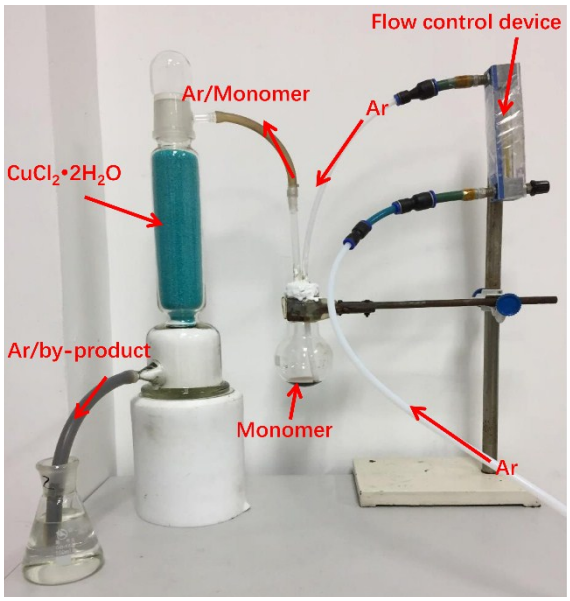

Fig. S1 Optical image of the reaction device.

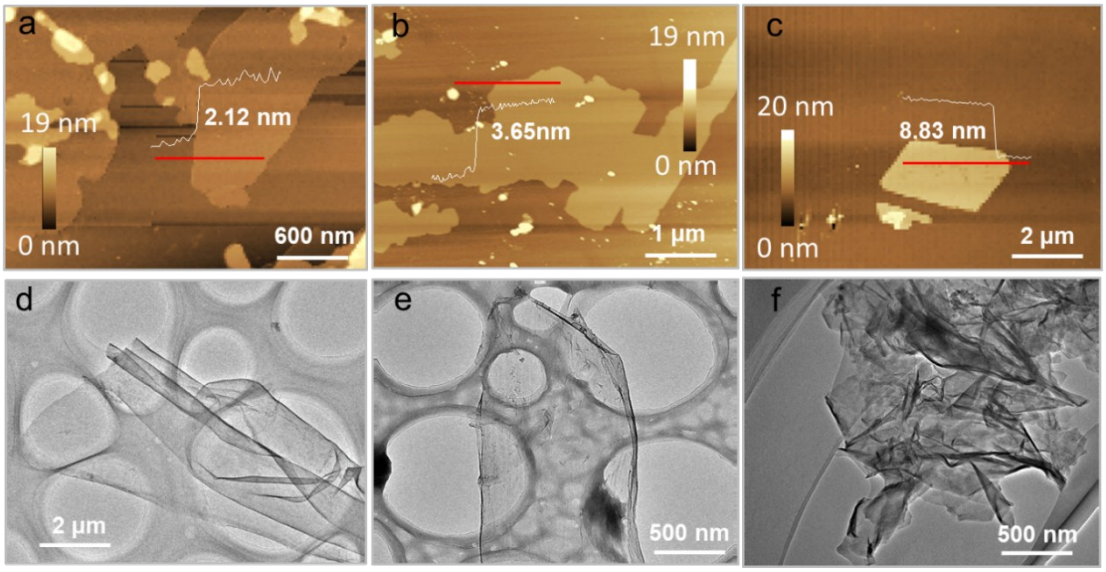

Fig. S2 (a), (b), (c) are AFM images for the thickness of ~2.1 nm, ~3.6 nm and ~8.8 nm under different reaction time of 5, 20, 60 min, respectively, respectively. (d), (e), (f) are corresponding TEM images for these nanosheets with different thickness.

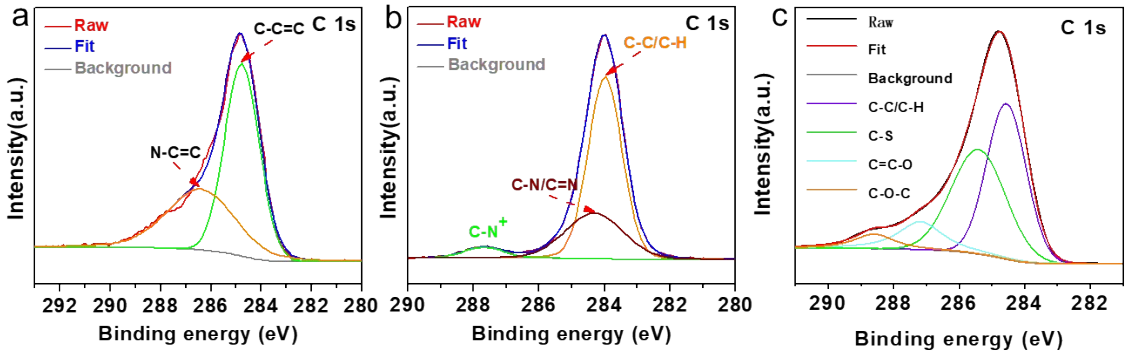

Fig. S3 (a) C1S spectra of PPy. The binding energy for C_α and C_β are centered at 285.11 and 284.50 eV, respectively [3-4]. Besides, 286.05 and 287.68 eV are responsible for C=N/C-N^+ and C=O bonds, respectively [4]. (b) C 1S spectra of the PANi. The peak located at 283.98 and 284.31 eV can be assigned to C-C/C-H and C-N/C=N bonds. Moreover, the binding energy at 399.72 eV corresponds to polaronic structures (C-$N^{\cdot+}$-) [5]. (c) C 1S spectra of the PEDOT. The four peaks at 284.56, 285.41, 287.18 and 288.59eV correspond to C-C/C-H, C-S, C=C-O and C-C-O bond [6], respectively.

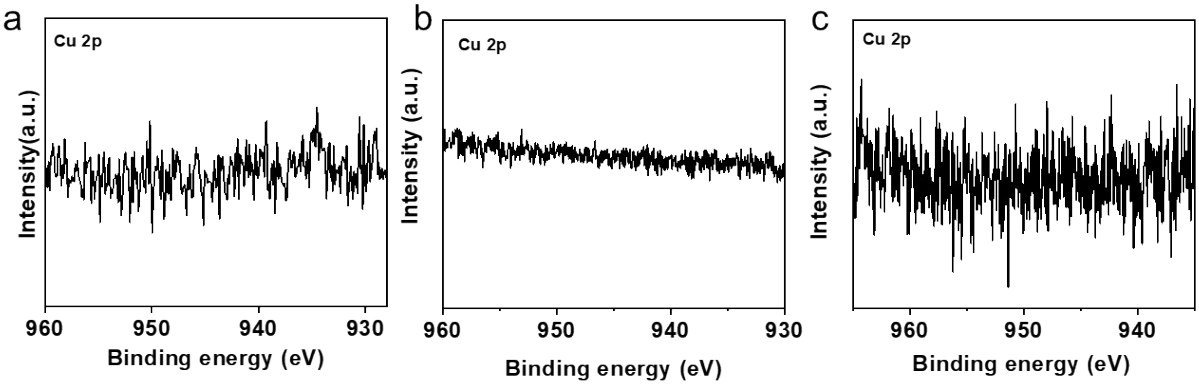

Fig. S4 XPS spectrums of Cu 2p for 2D PPy, 2D PANi and 2D PEDOT, respectively.

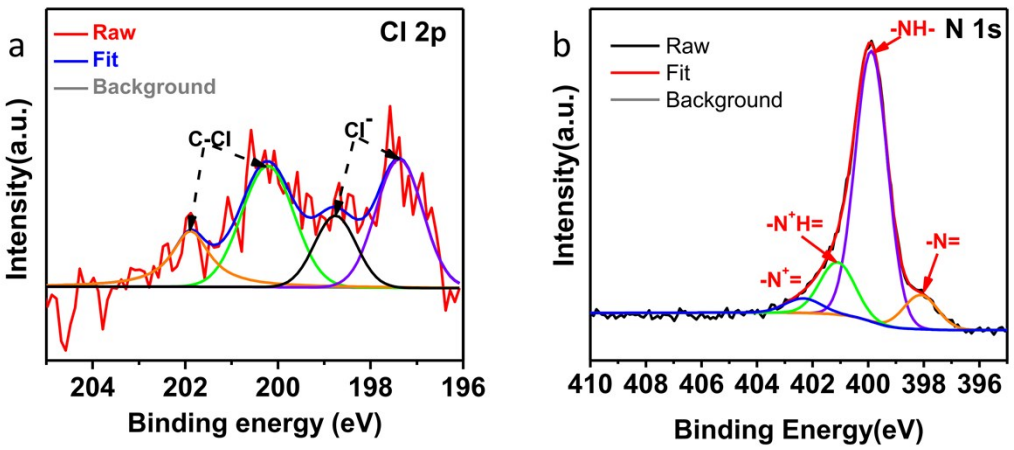

Fig. S5 (a) Cl 2p and N 1s XPS spectra of the PPy nanosheets. Fig. S5a illustrated the Cl^- doping to PPy chain skeleton. The binding energy centered at 197.38 and 198.76 eV are the Cl^- $2p_{1/2}$ and $2p_{3/2}$ peak, respectively. Meanwhile, the $2p_{1/2}$ and $2p_{3/2}$ peak of C-Cl bond are at 220.22 and 201.89 eV[5]. As shown in the Fig. S5b, the two peaks at 398.11 and 399.87 eV in the N 1s core level spectra for PPy are responsible for –N= and –NH– nitrogen atoms in the backbone of the PPy chain, respectively. The synthetic peaks located at 401.11 and 402.33 eV can be assigned to $–N^+H–$ cations and $–N^+=$ cations, which correspond to polarons[7-8].

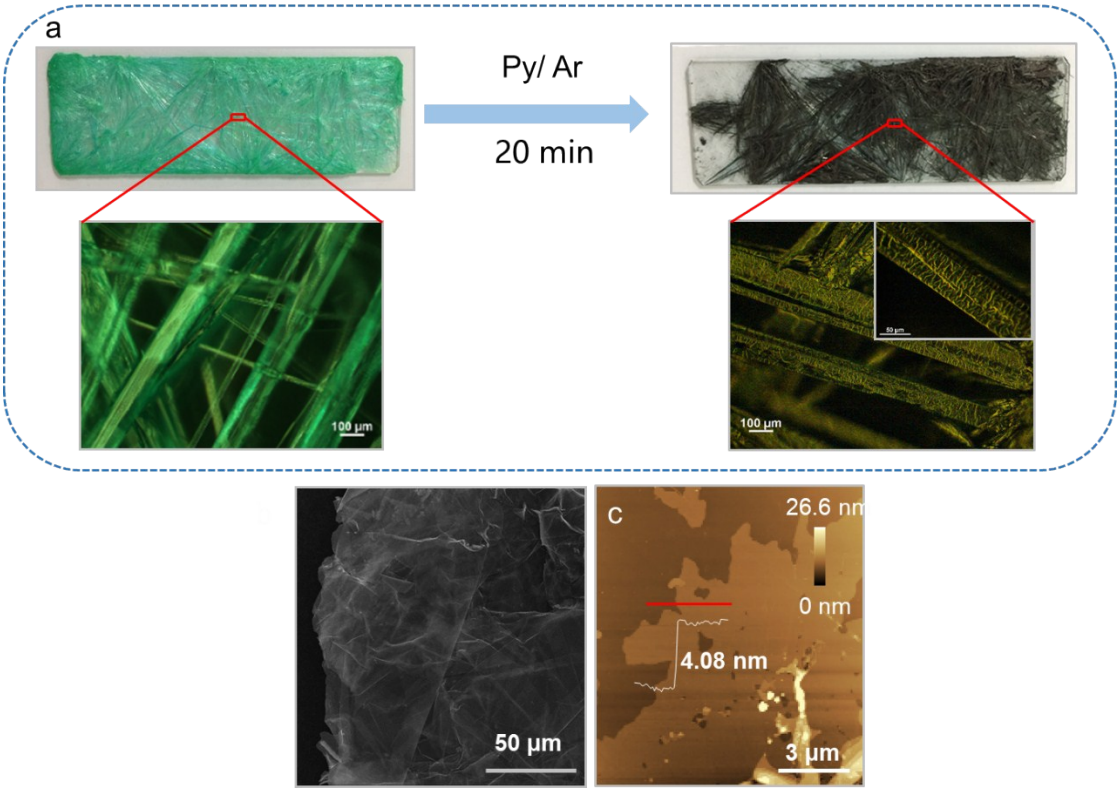

Fig. S6 (a) The Schematic diagram of the synthesis process. (b) SEM and (c) AFM of large 2D-PPy sheets, respectively.

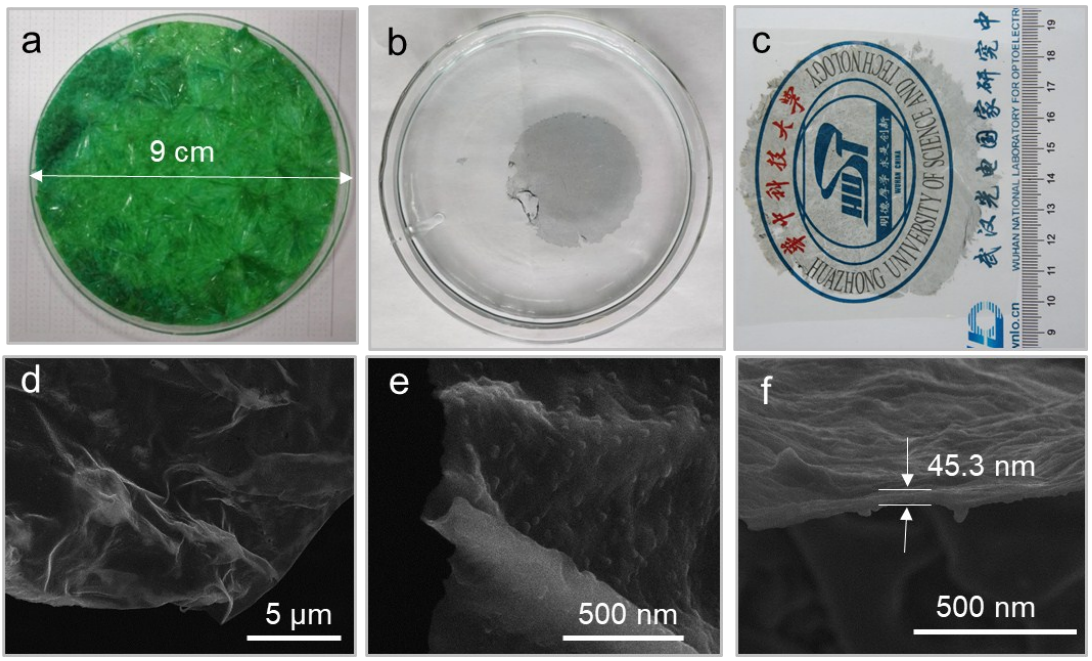

Fig. S7 (a) $CuCl_2 \cdot 2H_2O$ film in the culture dish. Optical image of large transparent PPy film in the water (b) and on the PET film (c). (d), (e) SEM and (f) cross-section image of the PPy film.

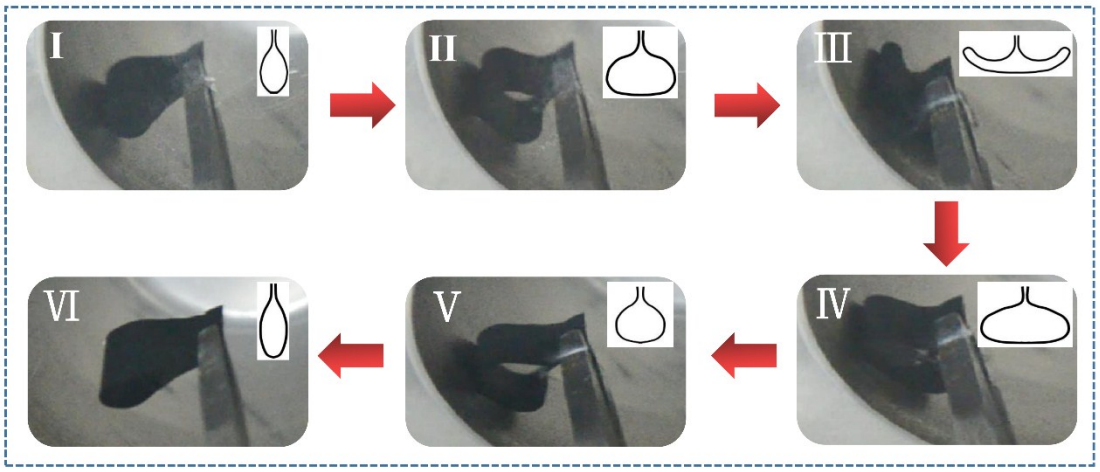

Fig. S8 The flexible 2D PPy assembled film can still keep flexibility in liquid nitrogen (-196 ℃) without any fragment under squeezed state.

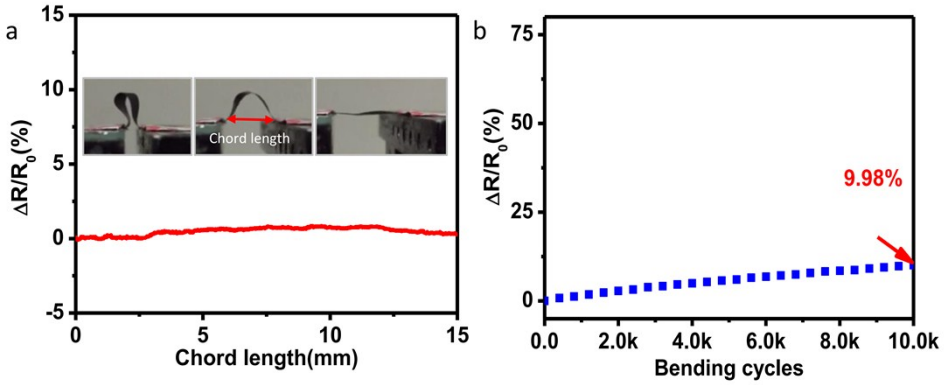

Fig. S9 (a) The electrical resistance changes of 2D PPy assembled film under different chord length. Inserts are the optical images of 2D PPy film with different chord length. (b) The electrical resistance changes after 10K bending cycles. The chord length can be converted to strain. The size of the film is 8.6 ×18.9 cm, and the thickness is 45 μm.

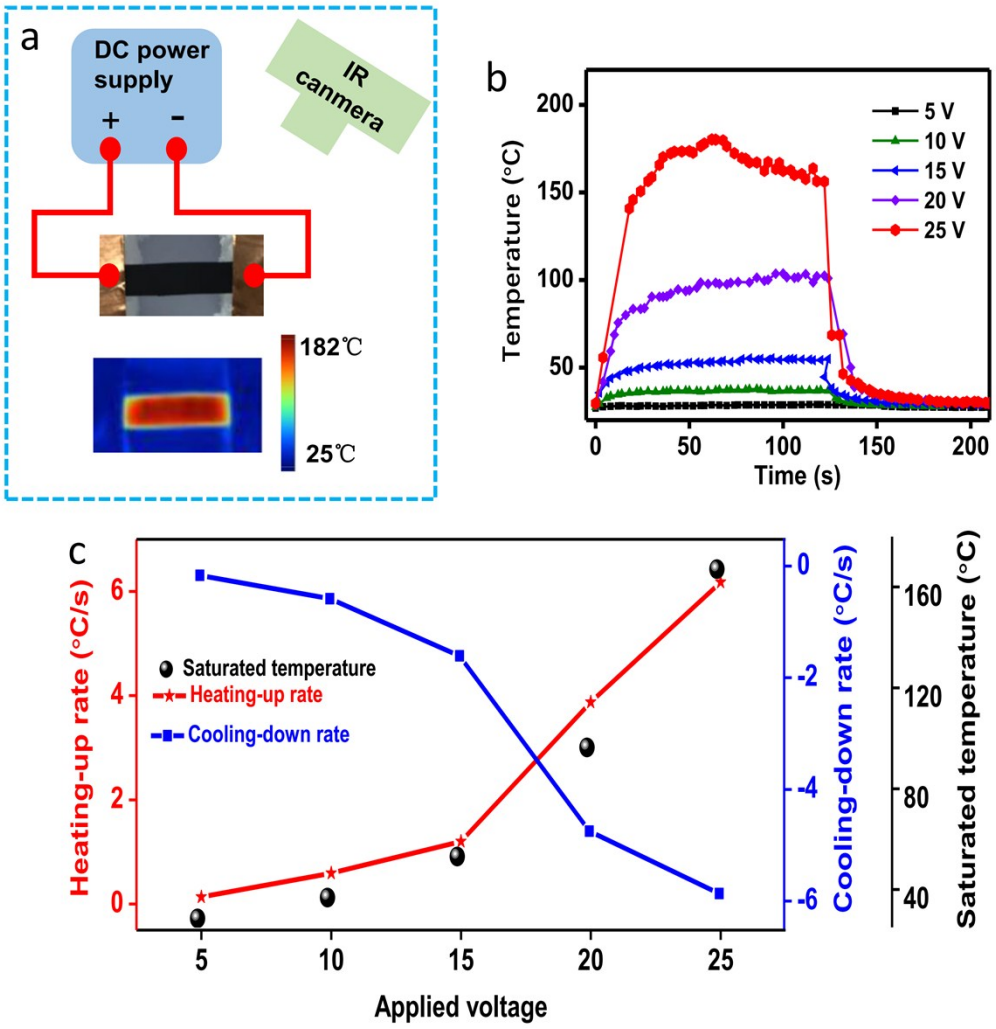

Fig. S10 (a) Diagram of experimental set-up for PPy-2 film electrothermal heaters, and the set-up below is the infrared pictures of 2 PPy-2 film at highest temperature. (b) Temperature profiles of PPy-2 film at different applied voltages. (c) Peak values of heating-up and cooling-down rates and the corresponding saturated temperatures as a function of applied voltage. In this experiment, the width and length of PPy film are as large as 0.5 and 1.25 cm, respectively. The highest temperature that PPy film is up to 182 °C, when the applied voltage is 25V. Besides, the highest heating-up and cool-down rate are 6 and -6 °C/s. Above all, the high conductivity of PPy film shows great joule heating performance.

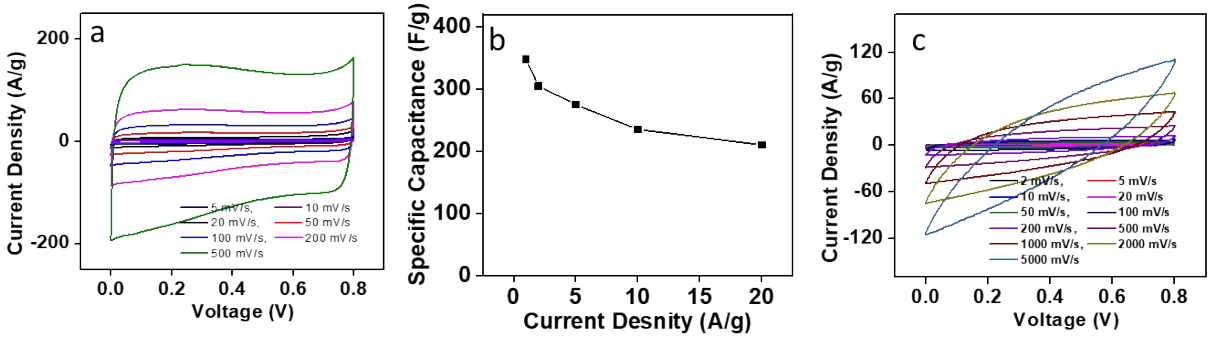

Fig. S11 (a) CV curves and (b) specific capacitance of PPy-1 electrode; (c) CV curves of PPy-2 electrode.

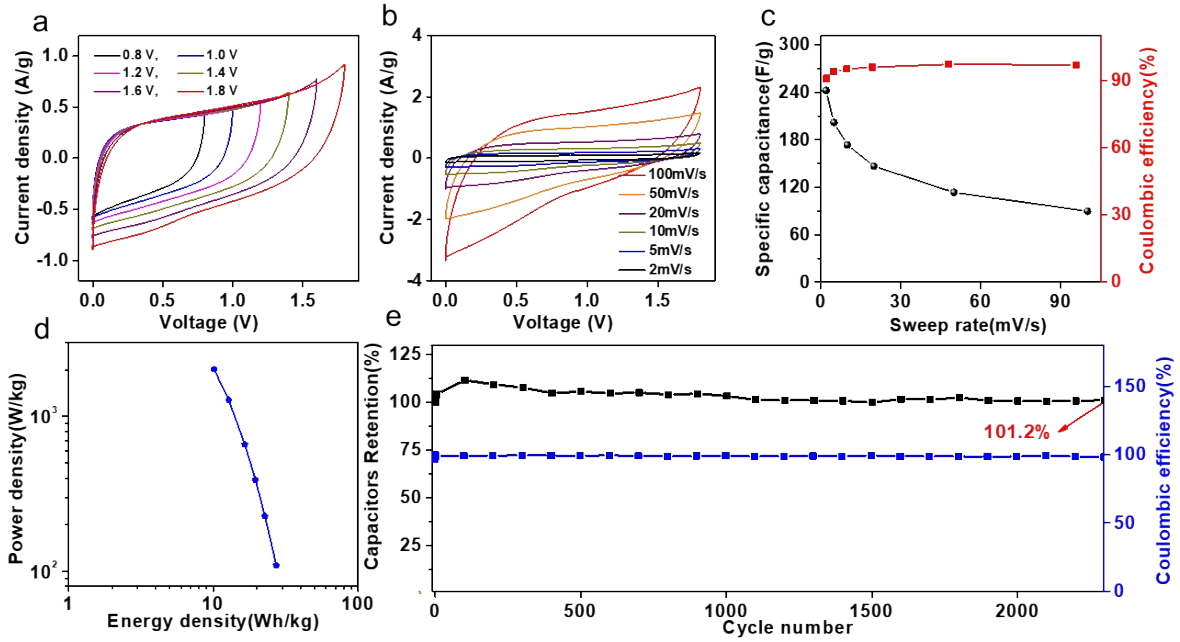

Fig. S12 (a)The CV curves of 2D PPy based organic device at scan rate of 20 mV/s with different operation voltage. (b) CV curves of 2D PPy based organic device at different scan rate. (c) The specific capacitance and coulombic efficiency of 2D PPy based organic device. (d) Ragone plots of 2D PPy based device; (e) the capacitance retention and coulombic efficiency of this device after 2300 cycles at 20 mV/s.

Table S1 The absorption peaks of FT-IR for 2D PPy nanosheets and their corresponding chemical bonds[1].

Chemical bond	Wavenumber（cm^{-1}）
C=C	1539.47
C-N(1)	1462.67
C-N(2)	1174.46
C-H(1)	1292.92
N-H	1041.41

Table S2 The absorption peaks of FT-IR for 2D PANi nanosheets and their corresponding chemical bonds[1].

Chemical bond	Wavenumber（cm^{-1}）
C=N	1640.32
C=C	1486.40
C-N	1281.57
C-H(1)	1067.47
C-H(2)	824.69

Table S3 The absorption peaks of FT-IR for 2D PEDOT nanosheets and their corresponding chemical bonds[2].

Chemical bond	Wavenumber（cm^{-1}）
C-C/C=C(1)	1644.52
C-C/C=C(2)	1542.20
C-C/C=C(3)	1457.07
C-O-C(1)	1279.31
C-O-C(2)	1159.54
C-O-C(3)	1045.41
C-S(1)	964.53
C-S(2)	841.74

Reference:

1. N. V. Blinova, J. Stejskal, M. Trchová, J. Prokeš, M. Omastová, *Euro. Poly. J.* **2007**, *43*, 2331.
2. A. Laforgue, L. Robitaille, *Macromol.* **2010**, *43*, 4194.
3. J. Joo, J. Lee, S. Lee, K. Jang, E. Oh, A. Epstein, *Macromol.* **2000**, *33*, 5131.
4. X. Wang, Y. Ma, X. Sheng, Y. Wang, H. Xu, *Nano Lett.* **2018**, *18*, 2217.
5. V. Jousseaume, M. Morsli, A. Bonnet, S. Lefrant, *J. Appl. Poly. Sci.* **1998**, *67*, 1209.
6. S. A. Spanninga, D. C. Martin, Z. Chen, *J. Phys. Chem. C* **2009**, *113*, 5585.
7. M. Vasquez, G. Cruz, M. Olayo, T. Timoshina, J. Morales, R. Olayo, *Polymer* **2006**, *47*, 7864.
8. L. Huang, X. Yao, L. Yuan, B. Yao, X. Gao, J. Wan, P. Zhou, M. Xu, J. Wu, H. Yu, *Energy Stor. Mater.* **2018**, *12*, 191.